Fibers and Polymers 2017, Vol.18, No.12, 2443-2453
DOI 10.1007/s12221-017-7479-y

ISSN 1229-9197 (print version)
ISSN 1875-0052 (electronic version)

Viscoelastic Modelling of Creep and Stress Relaxation Behaviour in PLA-PCL Fibres

Rui Miranda Guedes[1,2,3]*, Anurag Singh[1], and Viviana Pinto[2,3]

[1]*Department of Mechanical Engineering (DEMec), Faculty of Engineering of the University of Porto (FEUP), Porto 4200-465, Portugal*
[2]*INEGI - Laboratory of Optics and Experimental Mechanics, Porto 4200-465, Portugal*
[3]*LABIOMEP - Porto Biomechanics Laboratory – University of Porto, Porto 4200-450, Portugal*
(Received June 1, 2017; Revised September 14, 2017; Accepted September 24, 2017)

Abstract: In case of high performance athletes, ligaments are the most commonly injured tissues. Current gold standard process for replacement of ligament is autografting. Research in the field of biodegradable polymers (as a possible ligament device) has helped in overcoming the various drawbacks of autografting. Biodegradable blend of polylactic acid and polycaprolactone (PLA-PCL) have been proposed for use in a medical device to repair injured ligaments. By using a mathematical model, this study aims to characterise the non-linear viscoelastic properties of PLA-PCL fibres. In the present study, two modified models were used; the Burger's model and three-element standard solid model. The model parameters were calibrated by using the tensile and creep experimental data. In case of Burger's model, the parameters were significantly affected by the stress level. This functional stress dependency was represented by a second degree polynomial. By employing the previously computed parameters, the stress relaxation data of PLA-PCL fibres was used to check the model simulations. Only the predictions generated from the modified three-element standard solid model were found to be in an agreement with the experimental data. This model enables representing the general viscoelastic response of PLA-PCL fibres through a unique set of parameters.

Keywords: Biodegradable polymer, Finite deformation, Constitutive modelling, Non-linear viscoelasticity, Creep and stress relaxation

Introduction

Traditionally injured ligaments have been treated by using the biological grafts, namely autograft and allograft, which have good initial mechanical strength and can promote cell proliferation and new tissue growth. However, they possess limitations like limited availability, requirement of additional surgery for tissue harvest [1,2] restrictions in the movement is accompanied with pain, donor site scarcity, rejection by an immune induced response, elevated harvesting costs and diseases transfer [3]. Therefore, they do not provide long-term surgical alternative to this problem. The limitation of autografting may be resolved by utilizing biodegradable polymers as a potential device for ligament and it may help in overcoming the various drawbacks of autograft. The current solutions for soft tissues' replacement, based on biodegradable polymers, are prone to viscous effects which may lead to a premature failure of the device. Typically, these polymeric structures endure cyclic loading well above the linear elastic limit because of which they tend to accumulate permanent deformation [4,5]. An adept understanding of the mechanical behaviour is of uttermost importance to enhance the design of medical devices. Accordingly, a good knowledge of rheological phenomena, governing the mechanical behaviour of the polymeric structure, acquires a crucial importance.

*Corresponding author: rmguedes@fe.up.pt

The purpose of this work is to model the time-dependent behaviour of PLA-PCL fibres. These fibres possess the potential to be applied in fibrous scaffolds to grow soft tissues as ligaments and tendons [6]. Reliable qualitative and quantitative predictions of the macroscopic behaviour of these fibrous structures rely on a good knowledge of the mechanical behaviour of its basic constituents, i.e. the single fibre [7]. Biodegradable polymers can undergo failure much before the anticipated yield and ultimate tensile strength, due to its viscous nature, which leads to the creep or fatigue rupture. For example, in a study done by the Grabow *et al*. [5] significant creep deformation of polylactide (PLA) stents were reported when subjected to a constant load. This effect led to the strain accumulation and collapse of the stents. Soares conducted uniaxial tensile tests on PLLA fibres and confirmed the nonlinear viscoelastic characteristics of the PLLA fibres [8]. Christensen has associated this creep failure to the time-dependent kinetic crack growth in polymers [9].

Up to the proportionality limit, deformation occurring in the polymer specimen is like the uncoiling of the molecular chains. No intermolecular slippage is noticed and strains are recoverable in this area but only after a certain period. The deformation that occurs beyond this proportionality limit is unrecoverable. These distortions occur due to the actual displacement of the molecules over each other, which causes permanent deformation [10]. Constitutive modelling of the polymers can also be based on the molecular structure. However, the drawback of these models is their complexity

which makes determination of the parameters quite cumbersome. The inclusion of non-linear viscoelastic part is the key to defining the behaviour of polymer materials. Various approaches have been made in the past to include the nonlinear viscoelastic part. Hasanpour *et al*. [11] and Krishnaswamy *et al*. [12] developed a finite element algorithm to study nonlinear time-dependent problems. Liu *et al*. proposed modelling of PE based on creep testing at different stress levels [13]. Muliana proposed a model which was based on the Quasi-linear viscoelastic modelling by developing a nonlinear integral formulation [14]. Schapery constructed a one-dimensional nonlinear viscoelastic model which included four nonlinear parameters associated with the instantaneous, transient, loading rate and accelerated/ decelerated time-dependent responses, respectively [15].

Present work targets at analysing the non-linear behaviour of the PLA-PCL behaviour in the dry and saturated environment by using a modified Burger's model and the modified three-element standard solid model. The structure of the manuscript develops in the following manner. Experimental report the relevant material, experimental features along with the necessary explanation of constitutive models used in this study. Followed by the (uniaxial tensile tests and uniaxial creep and relaxation section) where the experimental results are analysed; creep stress and relaxation at different stress and strain levels are compared, respectively, along with saturation effect on the PLA-PCL fibres mechanical behaviour. Results and Discussion section reveal the parameters determined for both models and compare the model predictions with experimental data. The main conclusion drawn from this work is the remarkable capability of the modified three-element standard solid model to describe in a unique way the non-linear viscoelastic behaviour of PLA-PCL fibres.

Experimental

Material and Methods

All the experimental data presented were obtained previously by Martins *et al*. [16,17] and are briefly explained in the next sections. Data is provided in terms of engineering strain and engineering stress instead of true strain and true stress.

Chirmax provided PLA-PCL fibres with the blending ratio of 90:10 having number average molecular weight of 28000 g/mol and polydispersion index of 3.3. The glass transition temperature is 56 °C and the melting temperature is 157 °C. The diameter of the fibres is 0.5 mm and total length of the filament is 80 mm with 50 mm as gauge length. Three different PLA-PCL specimens were used to carry out a single test. Instron® ElectroPuls E1000 (High Wycombe, England) was used for mechanical tests on dry and saturated specimens.

Specimens' Saturation

For saturating the samples, a saline solution with 0.9 % NaCl was used. PLA-PCL fibres were soaked for at least 2 hours. During these tests, fibres were moistened using the dropper to ensure that they remained saturated throughout the mechanical tests. The saturated fibres were used to simulate the effect of human body environment.

Figure 1. PLA-PCL specimens.

Quasi-Static Loading

Tensile tests under displacement control with a displacement rate of 5 mm min^{-1} were set to achieve the strain rate around 15×10^{-4} s^{-1} at room temperature. The uniaxial experiments involved monotonic loading up to the point of failure; 2 kN load cell was used to measure the load. Figure 1 shows the PLA-PCL specimen used for the tests.

Uniaxial Creep and Relaxation Experiment

The PLA-PCL fibres were ramped up to required level for creep and relaxation tests. Then the fibres were kept at this level for 600 seconds and 300 seconds for creep and stress relaxation tests respectively. After the holding phase, fibres were unloaded in the next 600 seconds for creep tests and 300 seconds for stress relaxation tests.

Multi-step relaxation Test

Multi-step relaxation test with four different strain steps viz. at 4 % ε_{max}, 8 % ε_{max}, 12 % ε_{max}, and 16 % ε_{max} of maximum strain with a holding phase of 100 seconds at each strain level was conducted for dry specimens.

Constitutive Modelling

The Linear Viscoelastic theory is mostly valid in the small strain domain. Below certain stress levels, deformation behaviour is approximately linear. But with the increase in stress level, the material starts showing non-linear response [18]. In many applications, the material is subjected to high stress levels and strains well beyond the linear viscoelastic limit, exhibiting non-linear viscoelastic response. If enough time is given, a part of this inelastic deformation shows recovery. Both recoverable and permanent deformations are time dependent [19-24]. Understanding of these phenomena to model it correctly through mathematical equations is essential for the development of medical devices. There exist many classical mechanical models, which are being used to describe the time-dependent behaviour of the

polymers. These constitutive models have been developed in the past which are generally expressed through integral or differential equations to model the time-dependent mechanical behaviour of polymers [15,21-28].

Many of these differential equations based models are composed of one or several dashpots and Hookean elastic (spring) elements that simultaneously depict the viscous and elastic properties of the material. Different configurations of the spring and dashpot can be used to represent various constitutive models. Basic models such as Maxwell and Kelvin-Voigt are composed of a spring and dashpot element arranged in series and parallel respectively [22,23]. The models that are used to explain the viscoelastic beahavior of PLA-PCL fiberes are explained below.

Burger's Model

Burger's model has the Maxwell and Kelvin element connected in series. This model is one of the widely used models to represent the linear viscoelastic behaviour of polymers. Figure 2 shows the various elements of Burger's model.

For a linear viscoelastic solid, the total strain is the sum of three separate parts: ε_1 the immediate elastic deformation, ε_2 the delayed elastic deformation and ε_3 the Newtonian flow which is identical with the deformation of a viscous liquid obeying Newton's law of viscosity. The total strain as a function of time corresponds to the equation (1) [29]:

$$\varepsilon = \varepsilon_1 + \varepsilon_2 + \varepsilon_3 \tag{1}$$

The general constitutive equation of this model is as follows:

$$\sigma + \left(\frac{\eta_1}{R_1} + \frac{\eta_1}{R_2} + \frac{\eta_2}{R_1}\right)\dot{\sigma} + \frac{\eta_1\eta_2}{R_1R_2}\ddot{\sigma} = \eta_1\dot{\varepsilon} + \frac{\eta_1\eta_2}{R_2}\ddot{\varepsilon} \tag{2}$$

Equation (2) is a second order differential equation. The analytical solution for constant strain rate was deduced by Ebert *et al*. [23].

Under creep loading, if the applied stress σ_0 is constant, the solution to this equation gives the creep strain as follows:

$$\varepsilon = \sigma_0\left(\frac{1}{R_1} + \frac{1}{\eta_1} + \frac{1}{R_2}\left(1 - e^{\frac{-R_2 t}{\eta_2}}\right)\right) \tag{3}$$

In equation (3), t is the loading time, R_1 and η_1 are the modulus and viscosity of the Maxwell spring and dashpot respectively. R_2 and η_2 are the modulus and viscosity of the Kelvin spring and dashpot.

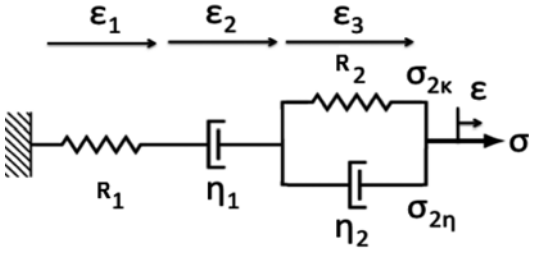

Figure 2. Spring and dashpot representation of Burger's model.

Modified Three-Element Standard Solid Model

The standard linear solid model, one of the classical viscoelastic model is composed of three elements; a Maxwell element connected in parallel with a linear spring [22,23]. In the work done by Khan *et al*., time and temperature dependent mechanical properties were explained by using a simple phenomenological viscoelastic model for polymers under finite deformations range [30]. The proposed model has Maxwell element connected in parallel with a Kelvin element having a non-linear spring. Uniaxial experimental data of stress-relaxation and monotonic loading at various strain rates were successfully analysed via the proposed model by Khan in his paper [30]. Furthermore, Zacharatos and Kontou modified the classical standard solid model to fit the data points by using fewer number of parameters than Khan *et al.* [31]. They considered the non-linear spring in parallel to the Maxwell element instead of Kelvin element as in Khan model. Here, Maxwell element is non-linear and has an Eyring dashpot in series along with the linear spring. Non-linear spring is dependent on the strain $\varepsilon(t)$. Figure 3 shows the representation of modified three element standard solid model using the spring and dashpot element along with the relation between non-linear spring E1 and Eyring dashpot. Zacharatos in his paper termed η_1 and η_2 as constants and they need to be determined by optimizing them with the experimental data [31]. In the earlier works, this viscosity was described as the function of strain rate. However, this viscosity function was originally proposed by Bird *et al.* [32] and has been modified ever since by other researchers based on the requirement of the polymeric behaviour [10,31,33,34].

From now on, for simplification purpose, the modified three-element standard solid model by Zacharatos will be referred as Kontou-Zacharatos model (K-Z model). K-Z model is proficient in describing the most important aspects of the viscoelastic behaviour of PLA-PCL fibres such as creep tests, stress-relaxation tests, quasi-static tests, along with multi-step relaxation experiments by the same model parameters.

Bardenhagen *et al*. [33] proposed a model for the finite deformation of the polymer by using differential constitutive

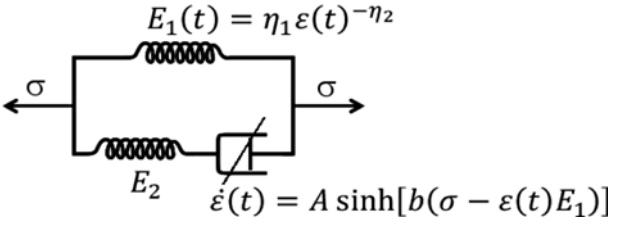

Figure 3. Schematic presentation of the K-Z model.

relations. They primarily focused on the generalisation of both viscoelastic and viscoplastic deformation region for the three-dimensional case.

The one-dimensional constitutive differential equation for the K-Z Model is as follows:

$$\dot{\sigma}(t) = (\eta_1 \varepsilon(t)^{-\eta_2} + E_2 - \eta_2 \eta_1 \varepsilon(t)^{-\eta_2})\dot{\varepsilon}(t) - AE_2 \sinh[b(\sigma(t) - \eta_1 \varepsilon(t)^{1-\eta_2})] \quad (4)$$

Under constant strain rate $\dot{\varepsilon}_0$, it becomes:

$$\dot{\sigma}(t) = (\eta_1 (t\dot{\varepsilon}_0)^{-\eta_2} + E_2 - \eta_2 \eta_1 (t\dot{\varepsilon}_0)^{-\eta_2})\dot{\varepsilon}_0 - AE_2 \sinh[b(\sigma(t) - \eta_1 (t\dot{\varepsilon}_0)^{1-\eta_2})] \quad (5)$$

Upon integrating the equation (5), analytical solution for this model is as follows:

$$\sigma(t) = \eta_1 \varepsilon^{1-\eta_2} - \frac{2}{b}\operatorname{arctanh}\left(\frac{A}{\dot{\varepsilon}_0} - \frac{\sqrt{\dot{\varepsilon}_0^2 + A^2}}{\dot{\varepsilon}_0}\tanh(E_2 bt\sqrt{\dot{\varepsilon}_0^2 + A^2}) + \operatorname{arctanh}\left(\frac{A}{\sqrt{\dot{\varepsilon}_0^2 + A^2}}\right)\right)\right) \quad (6)$$

Equation (6) can be written as a function of strain. Therefore, stress-strain quasi-static curve can be described as

$$\sigma(\varepsilon) = \eta_1 \varepsilon^{1-\eta_2} - \frac{2}{b}\operatorname{arctanh}\left(\frac{A}{\dot{\varepsilon}_0} - \frac{\sqrt{\dot{\varepsilon}_0^2 + A^2}}{\dot{\varepsilon}_0}\tanh(E_2 b\varepsilon/\dot{\varepsilon}_0\sqrt{\dot{\varepsilon}_0^2 + A^2}) + \operatorname{arctanh}\left(\frac{A}{\sqrt{\dot{\varepsilon}_0^2 + A^2}}\right)\right)\right) \quad (7)$$

where η_1, η_2, E_2, A and b are the material constants that are obtained after curve fitting the stress-strain experimental curve. Creep and stress relaxation experiments were used to verify the outreach of this model. Furthermore, to check the extent of the model, multi-step relaxation tests was also verified using this model.

Results and Discussion

Uniaxial Tensile Tests

The tensile properties of the samples were determined at room temperature. Young's modulus, tensile strength and elongation at break are listed in Table 1. Figure 4 shows the engineering stress-strain curve of PLA-PCL fibres under uniaxial tensile tests at the strain rate of 15×10^{-4} s^{-1} for dry and saturated specimens. Both the curves have two regions, region one (toe area) is very small as compared to the second region. The initial young's modulus was calculated from the toe area of the curve, which is below the yield point.

Table 1. Mechanical properties of dry and saturated PLA-PCL specimens

	Initial young modulus (MPa)	Elongation at break (%)	Tensile strength (MPa)
Dry specimen			
Specimen 1	1580	76.57	253.98
Specimen 2	1680	76.91	237.75
Specimen 3	1740	88.09	275.53
Average	1670	80.52	255.75
Saturated specimen			
Specimen 1	1500	79.67	242.59
Specimen 2	1470	77.40	232.51
Specimen 3	1360	77.58	232.22
Average	1440	78.21	235.77

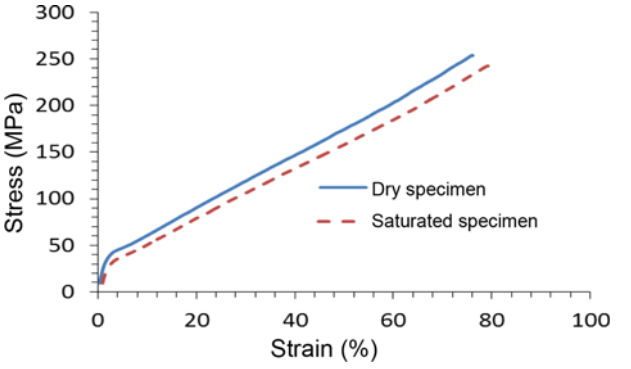

Figure 4. Engineering stress-strain curve for dry and saturated PLA-PCL specimens.

Young's modulus listed in Table 1 was calculated from the slope of the linear portion of the toe area.

Figure 4 and Table 1 display that how saturation has resulted in the decrease of the mechanical properties. Since saturation may have resulted in the increase of inter molecular spacing, this may lead to fibres getting soft. Consequently, the glass transition temperature will also drop, contributing to the reduction of mechanical properties.

Table 1 show the maximum stress and maximum strain values attained by the dry and saturated specimens before rupture. The values chosen for maximum strain and maximum stress were the lowest obtained in the tensile tests for a specimen at the expense of averaging values.

Uniaxial Creep and Relaxation

Table 2 shows the input stress/strain values for the creep and relaxation test for various levels. To define these tests, maximum stress and maximum strain values were obtained from the tensile tests.

For the creep test, dry PLA-PCL fibres suffer an increase in strain irrespective of the stress levels. Power law ($\sigma = a \times t^n$) is used to define the rate of creep by using the

Table 2. Stress input values for creep levels

Test label % $\sigma_{max}/\varepsilon_{max}$	Dry specimen	Saturated specimen
Creep Test - σ_{max}	237.75 MPa	232.22 MPa
T1 (15 % σ_{max})	35.66 MPa	34.83 MPa
T2 (30 % σ_{max})	71.32 MPa	69.67 MPa
T3 (45 % σ_{max})	106.99 MPa	104.50 MPa
T4 (60 % σ_{max})	142.65 MPa	139.33 MPa
Relaxation Test - ε_{max}	76.57 %	77.40 %
D1 (4 % ε_{max})	3.06 %	3.10 %
D2 (8 % ε_{max})	6.13 %	6.19 %
D3 (12 % ε_{max})	9.19 %	9.29 %
D4 (16 % ε_{max})	12.25 %	12.38 %

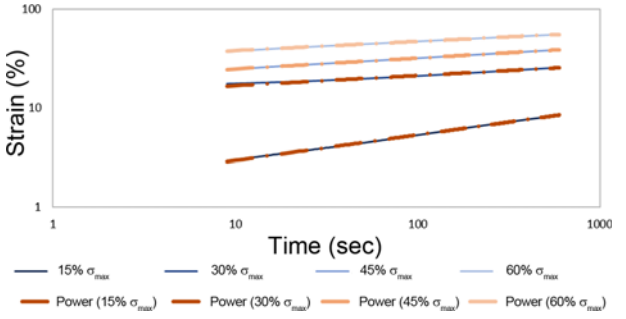

Figure 5. Linear portion of the creep curve on a log-log scale for the dry specimen.

most linear portion of the creep curve; rate of creep is the exponent (n) in the equation. Equation (8)-(11) shows that rate of creep is declining on increasing the stress levels, Figure 5 shows the linear portion of the creep curve on a log-log scale for the dry specimen.

$$\sigma = 15\ \%\ \sigma_{max};\ \varepsilon = 1.654 \times t^{0.2568};\ R^2 = 0.9996 \quad (8)$$

$$\sigma = 30\ \%\ \sigma_{max};\ \varepsilon = 11.764 \times t^{0.1058};\ R^2 = 0.9917 \quad (9)$$

$$\sigma = 45\ \%\ \sigma_{max};\ \varepsilon = 21.373 \times t^{0.098};\ R^2 = 0.9991 \quad (10)$$

$$\sigma = 60\ \%\ \sigma_{max};\ \varepsilon = 30.373 \times t^{0.0931};\ R^2 = 0.9995 \quad (11)$$

In addition, creep test for saturated PLA-PCL fibres show similar behaviour as that of dry specimens. However, there is a slight increase in the response of strain to the stress level. This behaviour is because of the saturation, as it results in softening of polymer and which has reflected with the increased strain levels. By using the power law, most linear portion of the creep curve is used to define the rate of creep (n). Equation (12)-(15) shows that the rate of creep is decreasing with the increase of stress levels, Figure 6 shows the linear portion of the creep curve on a log-log scale for saturated specimen.

$$\sigma = 15\ \%\ \sigma_{max};\ \varepsilon = 5.741 \times t^{0.1547};\ R^2 = 0.9937 \quad (12)$$

$$\sigma = 30\ \%\ \sigma_{max};\ \varepsilon = 14.837 \times t^{0.1224};\ R^2 = 0.9992 \quad (13)$$

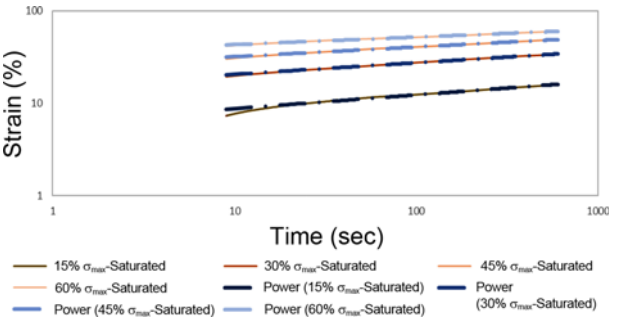

Figure 6. Linear portion of the creep curve on a log-log scale for the saturated specimen.

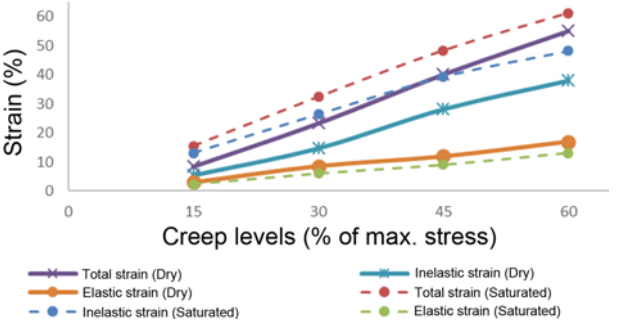

Figure 7. Various creep strain experienced during creep test for dry and saturated PLA-PCL specimens

$$\sigma = 45\ \%\ \sigma_{max};\ \varepsilon = 24.862 \times t^{0.1049};\ R^2 = 0.9977 \quad (14)$$

$$\sigma = 60\ \%\ \sigma_{max};\ \varepsilon = 36.539 \times t^{0.0813};\ R^2 = 0.9976 \quad (15)$$

By observing creep curves for dry and saturated specimens, the total strain was decomposed into elastic and inelastic strain. The elastic strain was measured after loading which when subtracted from the total strain gives the inelastic strain. Figure 7 displays the maximum strain attained by the specimens after 600 seconds for dry and saturated PLA-PCL fibres. From Figure 7 with the increase in creep levels, both the elastic and inelastic strain value increases. These values when compared with the saturated specimens showed larger deformation as already discussed above. Total strain experienced by the dry specimens was almost equivalent to the inelastic strain achieved in the case of saturation. While elastic strain for the saturated case was slightly lower than the dry specimen. For both these cases, the inelastic strain was a significant part of the total strain.

In case of stress relaxation, with the increase in strain levels there is an increase in the stress levels at least during the loading and holding phase. Power law is used to define the rate of relaxation by using the most linear portion of the stress relaxation curve; equations (16)-(19) show that rate of relaxation (n) first decreases and then it increases with the increasing levels of strain. Figure 8 shows the linear portion

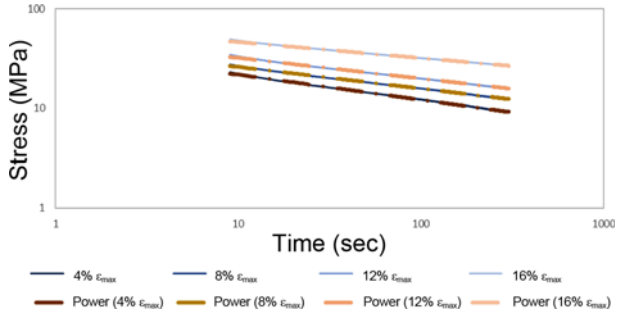

Figure 8. Linear portion of the stress relaxation curve on a log-log scale for the dry specimen.

of the stress relaxation curve on a log-log scale for the dry specimen.

$$\varepsilon = 4\ \%\ \varepsilon_{max};\ \sigma = 34.563 \times t^{-0.155};\ R^2 = 0.9984 \quad (16)$$

$$\varepsilon = 8\ \%\ \varepsilon_{max};\ \sigma = 44.51 \times t^{-0.280};\ R^2 = 0.9984 \quad (17)$$

$$\varepsilon = 12\ \%\ \varepsilon_{max};\ \sigma = 53.119 \times t^{-0.210};\ R^2 = 0.9996 \quad (18)$$

$$\varepsilon = 16\ \%\ \varepsilon_{max};\ \sigma = 64.853 \times t^{-0.173};\ R^2 = 0.9996 \quad (19)$$

For saturated PLA-PCL fibres, with the increase in strain levels there is an increase in the response of stress levels. When compared with the dry specimens, there response is slightly lower. Behaviour of saturated specimens were similar to the dry specimens. By using the power law, most linear portion of the relaxation curve is used to define the rate of relaxation (n). Equations (20)-(23) show that rate of relaxation first remains constant and then it increases with the increasing levels of strain. Figure 9 shows the linear portion of the stress relaxation curve on a log-log scale for the saturated specimen.

$$\varepsilon = 4\ \%\ \varepsilon_{max};\ \sigma = 31.995 \times t^{-0.285};\ R^2 = 0.9984 \quad (20)$$

$$\varepsilon = 8\ \%\ \varepsilon_{max};\ \sigma = 39.98 \times t^{-0.285};\ R^2 = 0.9991 \quad (21)$$

$$\varepsilon = 12\ \%\ \varepsilon_{max};\ \sigma = 52.261 \times t^{-0.277};\ R^2 = 0.9996 \quad (22)$$

$$\varepsilon = 16\ \%\ \varepsilon_{max};\ \sigma = 57.013 \times t^{-0.204};\ R^2 = 0.9976 \quad (23)$$

In case of relaxation, after certain period specimens seems

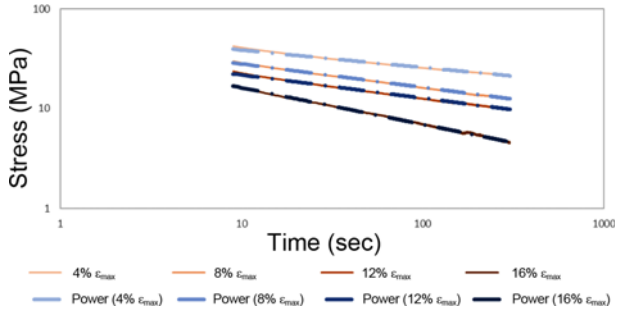

Figure 9. Linear portion of the stress relaxation curve on a log-log scale for the saturated specimen.

Table 3. Stress drop during stress relaxation experiments for dry and saturated PLA-PCL specimens

	Stress Relaxation Stress drop during stress relaxation experiments ($\Delta\sigma = \sigma_{max} - \sigma_{t=300\ sec}$)			
	4 % ε_{max}	8 % ε_{max}	12 % ε_{max}	16 % ε_{max}
Dry specimen	22.75	32.68	40.08	47.42
Saturated specimen	22.39	29.75	37.82	44.45

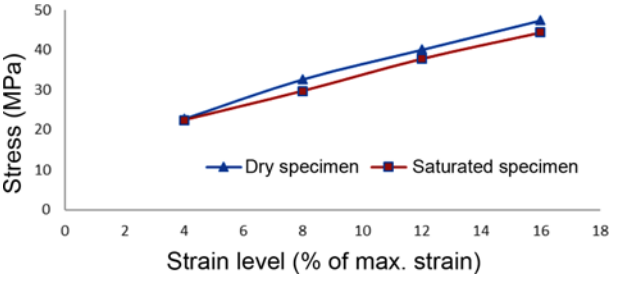

Figure 10. Stress drop during stress relaxation experiments.

to be reaching the equilibrium state both with dry and saturated specimens. This is defined as the stress-strain response near the zero-strain rate.

Table 3 and Figure 10 show the drop-in stress, defined as $\Delta\sigma = \sigma_{max} - \sigma_{t=300\ sec}$, during stress relaxation experiment from the point of maximum stress up to the point when unloading starts. During lowest strain loading, the drop is almost equal for both dry and saturated specimen. However, for the higher strain loading experiments, the difference in drop is nearly constant afterwards. Dry samples showed a larger drop in stress when compared with the saturated specimens. But for all the levels this difference remains constant.

Burger's Model

Burger's model is applied to creep experimental data. Table 4 shows the parameters obtained using the creep data and Figure 11 shows the result obtained by using the Burger's model with the creep data. These parameters were obtained from equation (3).

Good curve fitting of the experimental data was obtained when analysed separately for each stress level. The results are presented in Table 4 which indicates that the parameters R_1 and η_1 were significantly affected by the stress level. This effect was translated through functional dependency of the stress level, using a second-degree polynomial. The modulus of elasticity, R_1, was assumed to be constant below a stress threshold of 77.5 MPa becoming a function of stress, i.e. non-linear elastic above that threshold. The dashpot η_1 was assumed to have a non-Newtonian viscosity, becoming a function of stress. A similar approach was proposed and applied to describe the creep behaviour of an epoxy adhesive

Table 4. Burgers model parameters

Parameter	R_1 (MPa)	R_2 (MPa)	η_1 (1/MPa/s)	η_2 (1/MPa/s)
	$0.3696\sigma^2 - 68.14\sigma + 3460$, $\sigma \leq 77.5$ MPa 400, $\sigma > 77.5$ MPa	1300	$-0.0035386\sigma^2 + 0.9057\sigma + 32.50$	60000

Note: σ represents the applied stress in MPa.

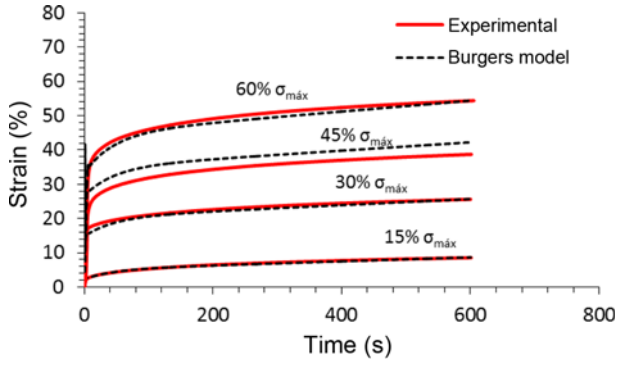

Figure 11. Modelling results for the first creep level (dry specimens).

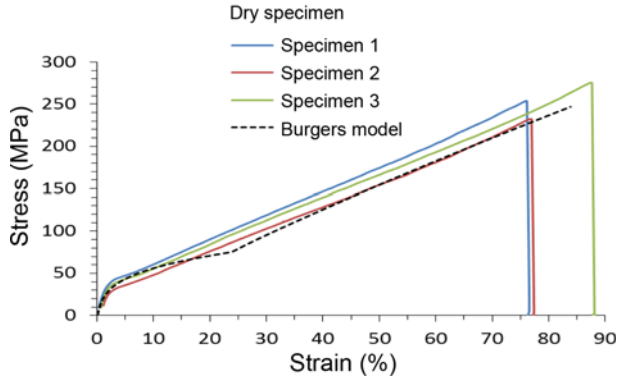

Figure 12. Correlation between the experimental data and the prediction of model for uniaxial tensile tests.

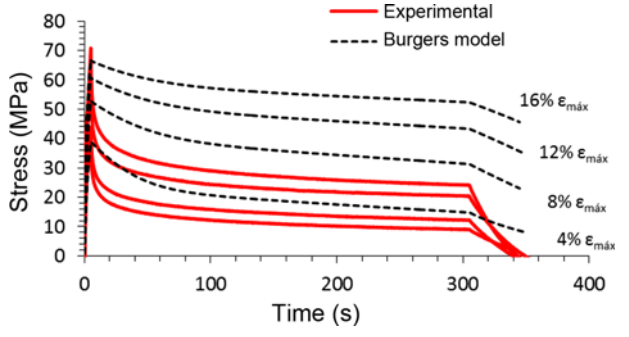

Figure 13. Burgers model prediction of relaxation behaviour (1st relaxation level, dry specimens).

[34]. Figure 12 compares the tensile test data with the model prediction. A discontinuity around the stress threshold of 77.5 MPa can be observed and is caused by the discontinuity on the first derivative of R_1 function.

The effectiveness of Burger's model is verified by using the stress relaxation experiment. The material parameters obtained from the creep tests were used to model the relaxation data. The model predictions do not agree with experimental data as shown in Figure 13. Model fails to capture the initial stress decay, as this decay is quite rapid.

In brief, the model was not able to predict the response of relaxation by using the parameters obtained from the creep tests. Therefore, this nonlinear viscoelastic model fails to describe the creep and stress relaxation in a unified manner, i.e. by using the same parameters. This is not the case of the non-linear viscoelastic model discussed in the next section.

K-Z Model

Equation (7) was used to obtain the material parameters for dry and saturated PLA-PCL specimen. Table 5 shows the material parameters obtained from engineering stress-strain data. After saturation, there is a slight decrease in some of the parameters. This change in parameters was expected, as saturation promotes modification of internal structure by changing the properties of material. Therefore, the alterations of the parameters were the reflection of these internal modifications.

Figure 14 and Figure 15 show the correlation of K-Z model with the dry tensile test data. Figure 16 shows the closer look at the initial data points; it shows the clear evidence that model can simulate the starting points as closely as the later points. The parameters obtained at the first place can be used to predict other loading cases. These correlation results show that the model is effectively able to simulate the tensile test results.

The model predictions of creep and stress relaxation response are shown in Figure 17 and Figure 18 respectively. For creep data, the model can simulate the experimental data successfully even at the higher stress level.

In the case of stress relaxation test, the model captures reasonably well the initial stress decay as it was very rapid. At higher strain level, there was a slight deviation from the experimental data. However, as these parameters were

Table 5. K-Z model parameter values

Material	Model parameter				
	η_1 (MPa)	η_2	E_2 (MPa)	A (1/s)	b (1/MPa)
PLA-PCL (dry)	290	-0.1	2200	0.00009	0.1
PLA-PCL (Saturated)	280	-0.1	1600	0.0002	0.1

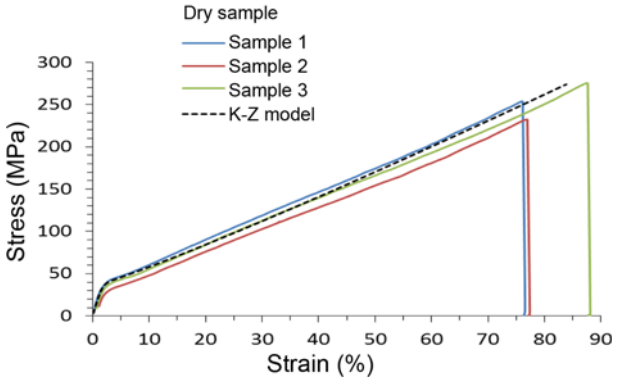

Figure 14. Correlation of K-Z model with the dry tensile tests data.

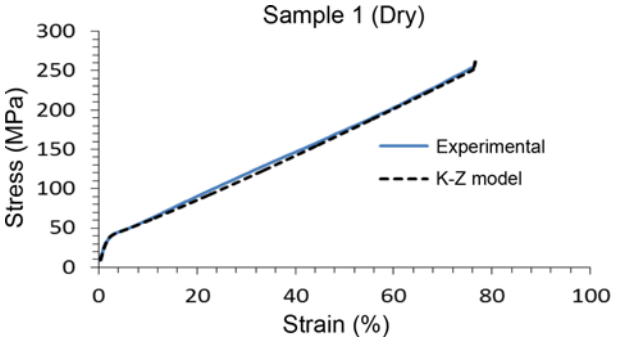

Figure 15. Correlation of K-Z model with the dry tensile tests data (sample 1).

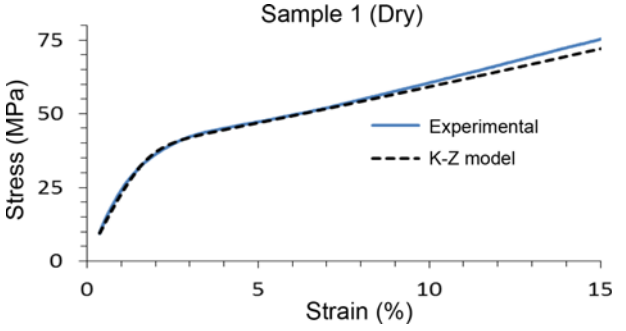

Figure 16. Correlation of K-Z model with the dry tensile tests data (initial data points).

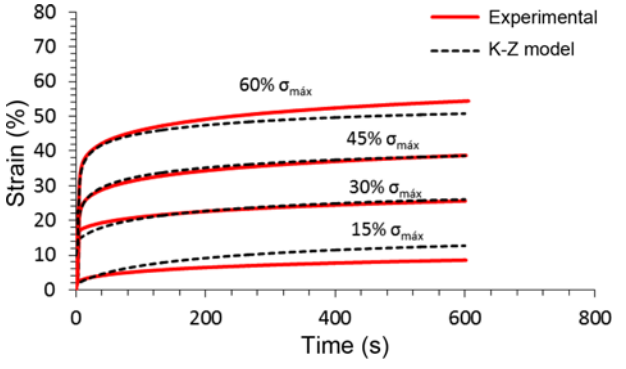

Figure 17. Comparison of experimental data and the model points for creep tests (dry specimen).

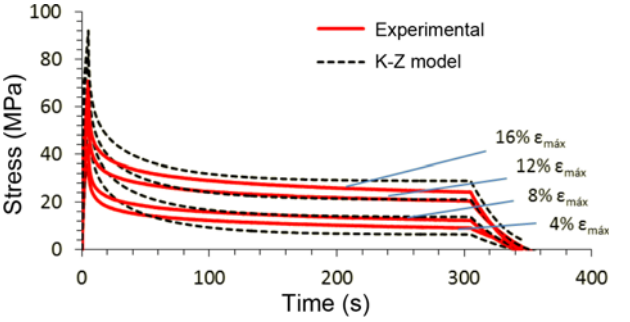

Figure 18. Comparison of experimental data and the model points for stress relaxation tests (dry specimen).

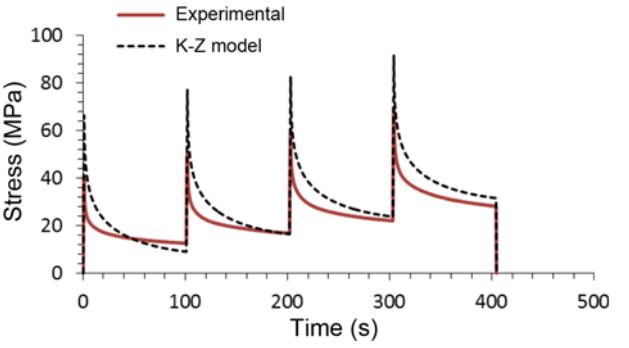

Figure 19. Comparison of multi-step relaxation test data and the model points (dry specimen).

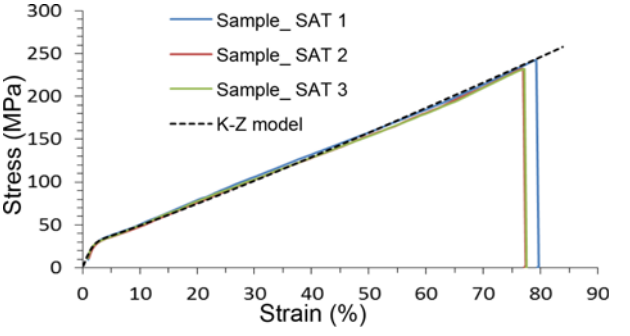

Figure 20. Correlation of K-Z model with the saturated tensile tests data.

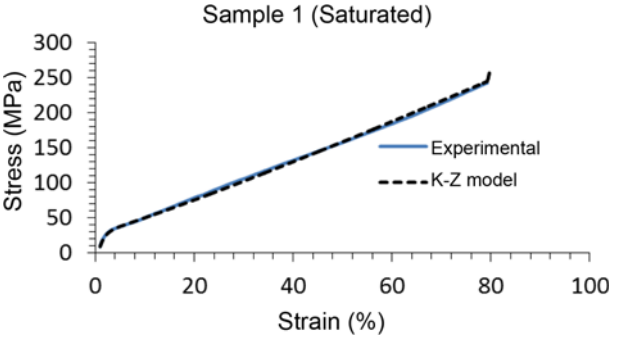

Figure 21. Correlation of K-Z model with the saturated tensile tests data (sample 1).

obtained from the quasi-static test, we can say that this non-linear viscoelasticity model is quite efficient in capturing mechanical behaviour of PLA-PCL fibres in a unified manner.

Furthermore, as seen in Figure 19 multi-step relaxation test was used to verify the extent of model. Behaviour of the model in capturing details of the test was far better than initially expected. These results have led to the conclusion that K-Z model is able to capture the details of different types of loadings by using the parameters from the quasi-static tests and is effective for the dry PLA-PCL fibres.

Figure 20 and Figure 21 compare K-Z model with the

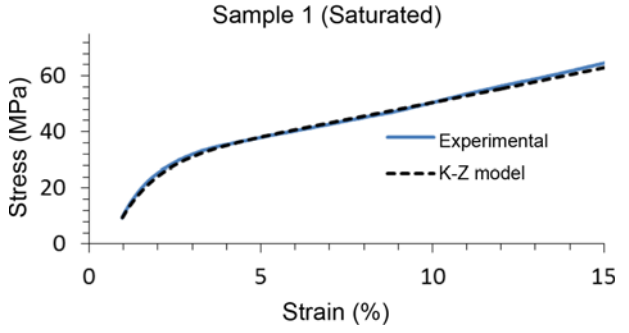

Figure 22. Correlation of K-Z model with the saturated tensile tests data (initial data points).

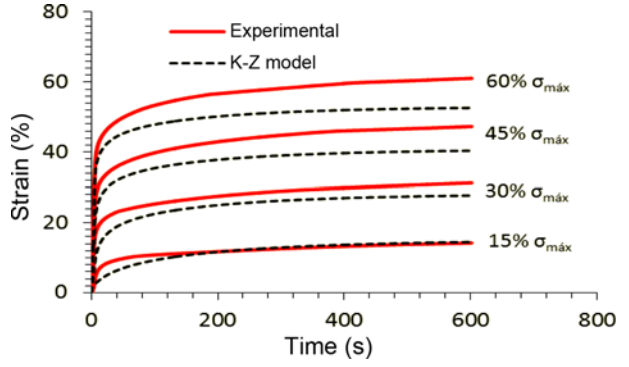

Figure 23. Comparison of experimental data and the model points for creep tests (saturated specimen).

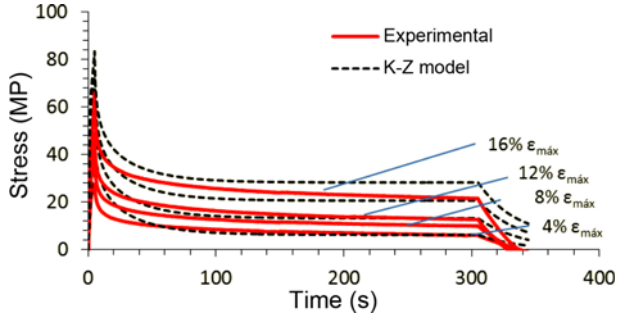

Figure 24. Comparison of experimental data and the model points for stress relaxation tests (saturated specimen).

tensile test data of saturated fibres. Saturation has resulted in the change of some of the parameters; these values are then used to simulate other experiments namely creep and stress relaxation tests. The model can capture the tensile test data points efficiently for saturated specimens. Figure 22 shows the closer look at the initial data points; it shows a clear evidence that model can effectively simulate the tensile test data.

Model parameters obtained from the quasi-static tests were then used to predict the creep response and stress relaxation behaviour as shown in Figure 23 and Figure 24 respectively. Saturation led to the modification of the elastic and viscoelastic properties. Additionally, as we go to higher stress levels, inelastic accumulation increases in the fibres. These effects were not so well captured by the model, leading to the deviation of experimental data and the predicted values at higher stress levels.

Again, in the case of stress relaxation tests, the model captures reasonably well the initial stress decay, despite it being very rapid. Also, at higher strain level there is a slight deviation from the experimental data. Upon the whole, the viscoelastic behaviour of saturated PLA-PCL fibres is still reasonably well captured by the K-Z model, as the model can simulate different types of loading by using the same parameters [31].

Earlier the attempts that were made to represent the non-linear behaviour of PLA-PCL fibres under large deformation were done by Laurent *et al.* [7], under the assumption that the PLA-PCL fibres obey elasto-plastic law. Vieira *et al.* [35] used hyperelastic models to capture the behaviour of PLA-PCL fibres at tensile loading, on the same note Soares *et al*. [36] used the power law generalized Neo-Hookean hyperelastic model, but for PLA fibres. In these cases, time dependent effects were ignored. Later, the time dependency effect was included by Vieira *et al*. [37] through the Bergström and Boyce model [38] This approach proved to be effective to capture the behaviour of PLA-PCL fibres subjected to cyclic tensile loading. However, this is a much more complex model than the hyperplastic models, which requires calibration of nine parameters. The work presented here is a continuation of pursuing a simpler model, the first approach was done using the linear viscoelastic Burgers' model [16]. Following that approach proved the necessity to non-linearize the model, which was done through the stress dependence of the material parameters in this work. Although it proved to be effective to represent creep and constant strain rate loading cases independently, but it does not represent the nonlinear viscoelastic effects of PLA-PCL fibres in a unified manner. In that regard K-Z model offers a superior performance, with reduced number of parameters to be calibrated (only five), along with a unified representation of the nonlinear viscoelastic response. Moreover, the one-dimensional K-Z model can also be developed for the three-dimensional case [30]. This approach was followed by

Berdenhagen *et al*. in his work by developing a three-dimensional model from the one-dimensional spring and dashpot model [33]. Since this model proved to possess the ability to represent the non-linear viscoelastic response in a unified manner, it can be used as a starting point for the three-dimensional generalisation.

Conclusion

This work presents a general methodology for constructing a uniaxial finite deformation constitutive modelling for polymeric fibre materials in the non-linear viscoelastic domain. Modified Burger's model and the K-Z model were used to simulate the experimental data for PLA-PCL fibres in dry and saturated state. Saturation resulted in the decrease of the mechanical properties by increasing the spacing between molecules which further softens these fibres. For both the cases, the inelastic strain is a significant part of the total strain. The rate of creep and rate of relaxation, both showed a decline with the increase in the level of stress and strain respectively.

Burger's model parameters were obtained from the creep test. The stress level has a significant impact on the parameters of the Maxwell element of the Burger's model. The model is modified to incorporate the stress influence by expressing the parameters as functions of the stress level. For verifying the model, stress relaxation experiments were used, which showed the inability of the model towards a unified representation of viscoelastic behaviour. However, for the case of K-Z model, parameters were determined by using the quasi-static tests to characterise the PLA-PCL behaviour. Upon the whole, K-Z model could simulate the creep, stress relaxation and multi-step relaxation behaviour by using the same set of parameters. In brief, K-Z model offers a simple and very flexible phenomenological approach to the modelling by employing less number of parameters than the Khan *et al*. model [30] and proved to be very effective in modelling the non-linear viscoelasticity response of PLA-PCL fibres in both states, dry and saturated. Therefore, this model can be utilised further to describe in unified manner the non-linear viscoelastic behaviour of PLA-PCL fibres.

Acknowledgement

Funding for this work was partially provided by FEDER, through Programa Operacional Factores de Competitividade - COMPETE, by national funding through FCT - Fundação para a Ciência e a Tecnologia, in the framework of project PTDC/EMEPME/114808/2009.

Viviana Pinto wants to thank FCT for PhD grant SFRH/BD/78749/2011.

Anurag Singh wants to thank "EUPHRATES", an Erasmus Mundus project led by the University of Santiago de Compostela (Spain) for the PhD scholarship.

References

1. D. Amiel, E. Billings, and F. L. Harwood, *J. Appl. Physiol.*, **69**, 902 (1990).
2. E. Bell, *Tissue Eng.*, **1**, 163 (1995).
3. D. W. Jackson, E. S. Grood, S. P. Arnoczkym, D. L. Butler, and T. M. Simon, *J. Sports. Med.*, **15**, 528 (1987).
4. A. C. Vieira, R. M. Guedes, and A. T. Marques, *J. Biomech.*, **42**, 2421 (2009).
5. N. Grabow, C. M. Bünger, K. Sternberg, S. Mews, K. Schmohl, and K.-P. Schmitz, *J. Med. Device.*, **1**, 84 (2007).
6. P. X. Ma, *Mater. Today*, **7**, 30 (2004).
7. C. P. Laurent, D. Durville, D. Mainard, J. F. Ganghoffer, and R. Rahouadj, *J. Mech. Behav. Biomed. Mater.*, **2**, 184 (2012).
8. J. S. Soares, "Constitutive Modeling for Biodegradable Polymers for Applications in Endovascular Stents", 2008.
9. R. M. Christensen, *Mech. Time-Dependent Mater.,* **8**, 1 (2004).
10. A. Plaseied and A. Fatemi, *J. Mater. Sci.,* **43**, 1191 (2008).
11. K. Hasanpour, S. Ziaei-Rad, and M. Mahzoon, *Int. J. Plast.*, **25**, 1154 (2009).
12. P. Krishnaswamy, M. E. Tuttle, A. F. Emery, and J. Ahmad, *Polym. Eng. Sci.*, **32**, 1086 (1992).
13. H. Liu, M. A. Polak, and A. Penlidis, *Polym. Eng. Sci*., **48**, 159 (2008).
14. A. Muliana, *Int. J. Solids Struct.*, **51**, 122 (2014).
15. R. A. Schapery, *Polym. Eng. Sci.*, **9**, 295 (1969).
16. C. Martins, V. Pinto, R. M. Guedes, and A. T. Marques, *Procedia Engineering,* **114**, 768 (2015).
17. C. Martins, M.Sc. Dissertation, Faculdade de Engenharia da Universidade do Porto, 2014.
18. G. Dean, L. Crocker, B. Read, and L. Wright, *Int. J. Adhes. Adhes.*, **24**, 295 (2004).
19. A. D. Drozdov, "Finite Elasticity and Viscoelasticity: A Course in the Non-linear Mechanics of Solids", p.238, World Scientific, 1996.
20. A. D. Drozdov, "Viscoelastic Structures: Mechanics of Growth and Aging", p.171, Academic Press, 1998.
21. J. D. Ferry, "Viscoelastic Properties of Polymers", p.73, John Wiley & Sons, 1980.
22. W. N. Findley, J. S. Lai, and K. Onaran, "Creep and Relaxation of Nonlinear Viscoelastic Materials", p.2, Dover Publications, Inc., New York, 1989.
23. C. Ebert, W. Hufenbach, A. Langkamp, and M. Gude, *Polymer Testing*, **30**, 183 (2011).
24. R. S. Lakes, "Viscoelastic Solids", p.44, CRC Press, 1998.
25. A. D. Drozdov and A. L. Kalamkarov, *Polym. Eng. Sci.*, **36**, 1907 (1996).
26. Y. A. Rossikhin and M. V. Shitikova, *Comput. Math. with Appl.,* **66**, 755 (2014).
27. P. Provenzano, R. Lakes, T. Keenan, and R. Vanderby, Jr.,

Ann. Biomed. Eng., **29**, 908 (2001).
28. A. D. Drozdov, *Mech. Res. Commun.,* **25**, 83 (1998).
29. X. Liu, S. Zhang, X. J. Xu, Z. Zhang, L. Zhou, and G. Zhang, *Fiber. Polym*., **14**, 1635 (2013).
30. A. S. Khan, O. Lopez-Pamies, and R. Kazmi, *Int. J. Plast.,* **22**, 581 (2006).
31. A. Zacharatos and E. Kontou, *J. Appl. Polym. Sci.,* **132**, 1 (2015).
32. R. B. Bird, R. C. Armstrong, and O. Hassanger, "Dynamics of Polymeric Liquids", Vol. 1, p.169, Fluid Mechanics 1987.
33. S. G. Bardenhagen, M. G. Stout, and G. T. Gray, *Mech. Mater.*, **25**, 235 (1997).
34. P. Majda and J. Skrodzewicz, *Int. J. Adhes. Adhes.*, **29**, 396 (2009).
35. A. C. Vieira, J. C. Vieira, J. M. Ferra, F. D. Magalhães, R. M. Guedes, and A. T. Marques, *J. Mech. Behav. Biomed. Mater*., **4**, 451 (2011).
36. J. S. Soares, K. R. Rajagopal, and J. E. Moore, *Biomech. Model. Mechanobiol.*, **9**, 177 (2010).
37. A. C. Vieira, R. M. Guedes, and V. Tita, *Int. J. Solids Struct.*, **51**, 1164 (2014).
38. J. Bergström and M. Boyce, *J. Mech. Phys. Solids,* **46**, 931 (1998).